

**Special Section:**

Forum for Arctic Modeling and Observational Synthesis (FAMOS) 2: Beaufort Gyre phenomenon

Key Points:

- Introduction to the FAMOS-2 special collection with papers mainly on studies in the region of the Arctic Ocean's Beaufort Gyre
- Physical, geochemical, biological, and ecosystem components of the Beaufort Gyre system are investigated
- New observations, ideas, and hypotheses revealing mechanisms influencing the Beaufort Gyre are discussed

Supporting Information:

- Supporting Information S1

Correspondence to:

A. Proshutinsky,
aproshutinsky@whoi.edu

Citation:

Proshutinsky, A., Krishfield, R., & Timmermans, M.-L. (2020). Introduction to special collection on arctic ocean modeling and observational synthesis (FAMOS) 2: beaufort gyre phenomenon. *Journal of Geophysical Research: Oceans*, 125, e2019JC015400. <https://doi.org/10.1029/2019JC015400>

Received 18 JUN 2019

Accepted 7 JUL 2019

Accepted article online 12 JUL 2019

©2019. The Authors.

This is an open access article under the terms of the Creative Commons Attribution-NonCommercial-NoDerivs License, which permits use and distribution in any medium, provided the original work is properly cited, the use is non-commercial and no modifications or adaptations are made.

Introduction to Special Collection on Arctic Ocean Modeling and Observational Synthesis (FAMOS) 2: Beaufort Gyre Phenomenon

A. Proshutinsky¹ , R. Krishfield¹ , and M.-L. Timmermans²

¹Woods Hole Oceanographic Institution, Woods Hole, MA, USA, ²Geology and Geophysics Department, Yale University, New Haven, CT, USA

Abstract One of the foci of the Forum for Arctic Modeling and Observational Synthesis (FAMOS) project is improving Arctic regional ice-ocean models and understanding of physical processes regulating variability of Arctic environmental conditions based on synthesis of observations and model results. The Beaufort Gyre, centered in the Canada Basin of the Arctic Ocean, is an ideal phenomenon and natural laboratory for application of FAMOS modeling capabilities to resolve numerous scientific questions related to the origin and variability of this climatologic freshwater reservoir and flywheel of the Arctic Ocean. The unprecedented volume of data collected in this region is nearly optimal to describe the state and changes in the Beaufort Gyre environmental system at synoptic, seasonal, and interannual time scales. The in situ and remote sensing data characterizing ocean hydrography, sea surface heights, ice drift, concentration and thickness, ocean circulation, and biogeochemistry have been used for model calibration and validation or assimilated for historic reconstructions and establishing initial conditions for numerical predictions. This special collection of studies contributes time series of the Beaufort Gyre data; new methodologies in observing, modeling, and analysis; interpretation of measurements and model output; and discussions and findings that shed light on the mechanisms regulating Beaufort Gyre dynamics as it transitions to a new state under different climate forcing.

1. Introduction

Since organization of the Arctic Ocean Model Intercomparison Project (AOMIP) in 1999 and later in the FAMOS and FAMOS-2 projects, the Beaufort Gyre theme has dominated the major coordinated studies of the AOMIP/FAMOS international community. Specifically, under the FAMOS project umbrella, the Beaufort Gyre circulation cell centered in the Canada Basin of the Arctic Ocean has become an ideal phenomenon and natural laboratory for application of FAMOS numerical simulation capabilities to validate and calibrate models and to resolve numerous scientific questions related to the origin and variability of this climatological freshwater reservoir and flywheel system of the Arctic Ocean.

Fresh water accumulation in the Beaufort Gyre region (Figure 1) is a principal dynamical and thermodynamical process, reflecting numerous complicated relationships among the atmosphere, sea ice, ocean, and ecosystems. Scientific interest in the Arctic freshwater budget has been growing since the pioneering work of Aagaard and Carmack (1989), who estimated the Arctic Ocean freshwater content based on data from the 1950s to 1980s. In the 1990s, the mapping of Arctic Ocean freshwater content and identification of the sources and sinks of fresh water were continued (see the set of papers in Lewis, 2000). In the 2000s, research shifted toward modeling of the salinity minimum in the Beaufort Gyre region (e.g. Steele et al., 2001), and identification of processes responsible for fresh water accumulation and release (e.g., Proshutinsky et al., 2002), as well as investigation of connections between the Beaufort Gyre system and Sub-Arctic regions (e.g., Armitage et al., 2016; Carmack et al., 2016; Dukhovskoy et al., 2004, 2006a, 2006b; Proshutinsky, Krishfield, & Barber, 2009; see also Proshutinsky, Krishfield, Timmermans, et al., 2009; Proshutinsky et al., 2002; Proshutinsky et al., 2015; Rabe et al., 2011, 2014; and Timmermans et al., 2011). At the same time, several coupled ice-ocean numerical modeling studies have simulated Arctic Ocean freshwater content variability, freshwater fluxes between the Arctic Ocean and North Atlantic, and Beaufort Gyre freshwater content (e.g., Condron et al., 2009; Proshutinsky et al., 2011).

Recently, there has been a focus on explaining factors and mechanisms responsible for fresh water accumulation, release, and saturation in the Beaufort Gyre region (e.g., based on observations (Giles et al.,

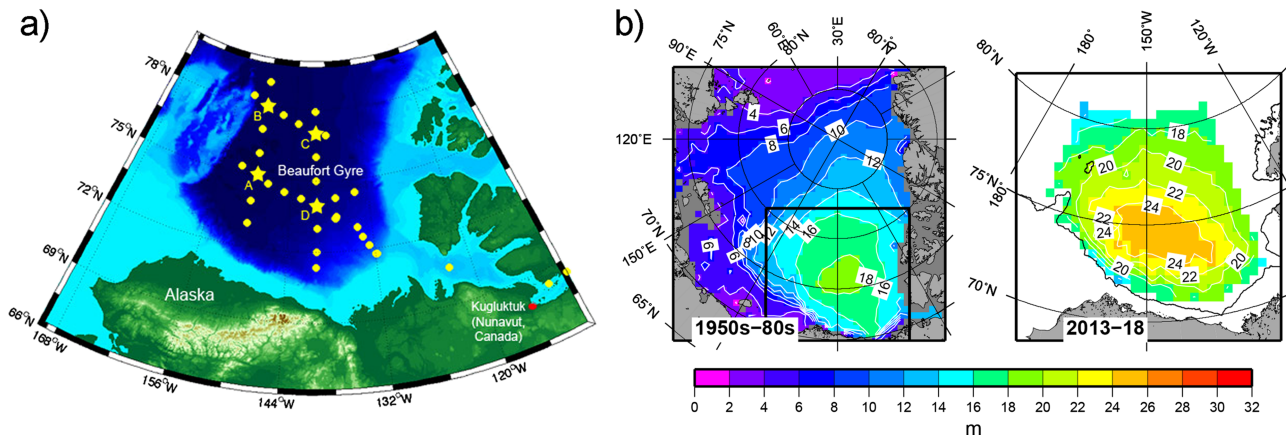


Figure 1. (a) Beaufort Gyre region with Beaufort Gyre Observational System (BGOS) mooring locations depicted as stars (moorings A-D), and sites of standard CTD stations where observations of sea ice and water physical and geochemical parameters have been conducted over the period 2003-2018. (b) Time-averaged summer freshwater content (in meters, relative to reference salinity 34.8; colors and contours) in the Beaufort Gyre region for 1950s-1980s and 2013-2018.

2012; Haine et al., 2015; Krishfield et al., 2014; McLaughlin et al., 2011) and modeling (Lique et al., 2016; Marshall et al., 2017; Nummelin et al., 2016). The papers comprising this special collection continue these investigations using new observations, ideas, and hypotheses to reveal mechanisms of changes and major factors influencing dynamics and thermodynamics of the Beaufort Gyre phenomenon.

1.1. Beaufort Gyre System Definition and Climatology

The Beaufort Gyre is a complex Arctic regional climate system (e.g., Proshutinsky, Krishfield, & Timmermans, 2009) including the atmosphere, sea ice, and ocean (Figure 2). The hydrography has a multi-layer structure (Figure 3) driven by strong dynamic and thermodynamic processes that interplay during the seasonal cycle and from year to year. The typical vertical water mass temperature (T) and salinity (S) structure (Figure 3) at the center of the maximum freshwater content (coinciding with the center of geostrophic circulation pattern) can be described in terms of five distinctive oceanic layers: a mixed layer with water S and T changing seasonally with large magnitudes depending mainly on sea ice conditions and wind forcing, Pacific origin summer and winter layers, and Atlantic origin and deep ocean layers.

The region is forced by seasonal variability, such as intraannual changes of wind sense and speed (strongly anticyclonic in winter and relatively weak cyclonic in summer, e.g., Proshutinsky, Krishfield, & Barber, 2009; Proshutinsky, Krishfield, Timmermans, et al., 2009; Proshutinsky et al., 2002, and see Figure 2, top panels) and changes in insolation from around 500 W/m^2 in summer to complete darkness in winter (Overland, 2009). In addition, the water-mass layers of the Beaufort Gyre depend on the availability of fresh water in the upper ocean from sea ice growth/melt, and from river runoff and net precipitation. One more external factor influencing water properties in the Beaufort Gyre is a significant sea level (pressure) gradient between the Pacific and Atlantic Ocean, which together with regional wind regulates the Bering Strait water inflow to the Arctic Ocean from the Pacific Ocean. Water T and S and volume of the Pacific water layer depend substantially on the magnitude of this pressure gradient. This inflow of Pacific water (more saline than the Beaufort Gyre mixed layer, and seasonally modified by surface buoyancy fluxes over the Chukchi Sea region) is the major source of fresh water and heat for the halocline in the Beaufort Gyre region.

In climatological data from the 1980s-2010s, the Beaufort Gyre is clearly recognizable as an anticyclonic circulation cell in the Canada Basin represented in sea level atmospheric pressure and geostrophic wind patterns, sea ice motion, sea surface heights, and surface geostrophic circulation (Figure 2) known from observations. Important new understanding of atmosphere-ice-ocean relationships in the region are discussed by Mahoney et al. (2019), Lewis and Hutchings (2019), and Heorton et al. (2019) in this special collection.

The boundaries of the Beaufort Gyre (Figure 2, yellow region; see also Figure 1) were first specified based on the regional freshwater content distribution observed in 2003-2007 (Proshutinsky, Krishfield, Timmermans, et al., 2009). Regan et al. (2019, this special collection) analyze changes of the Beaufort Gyre location, extent,

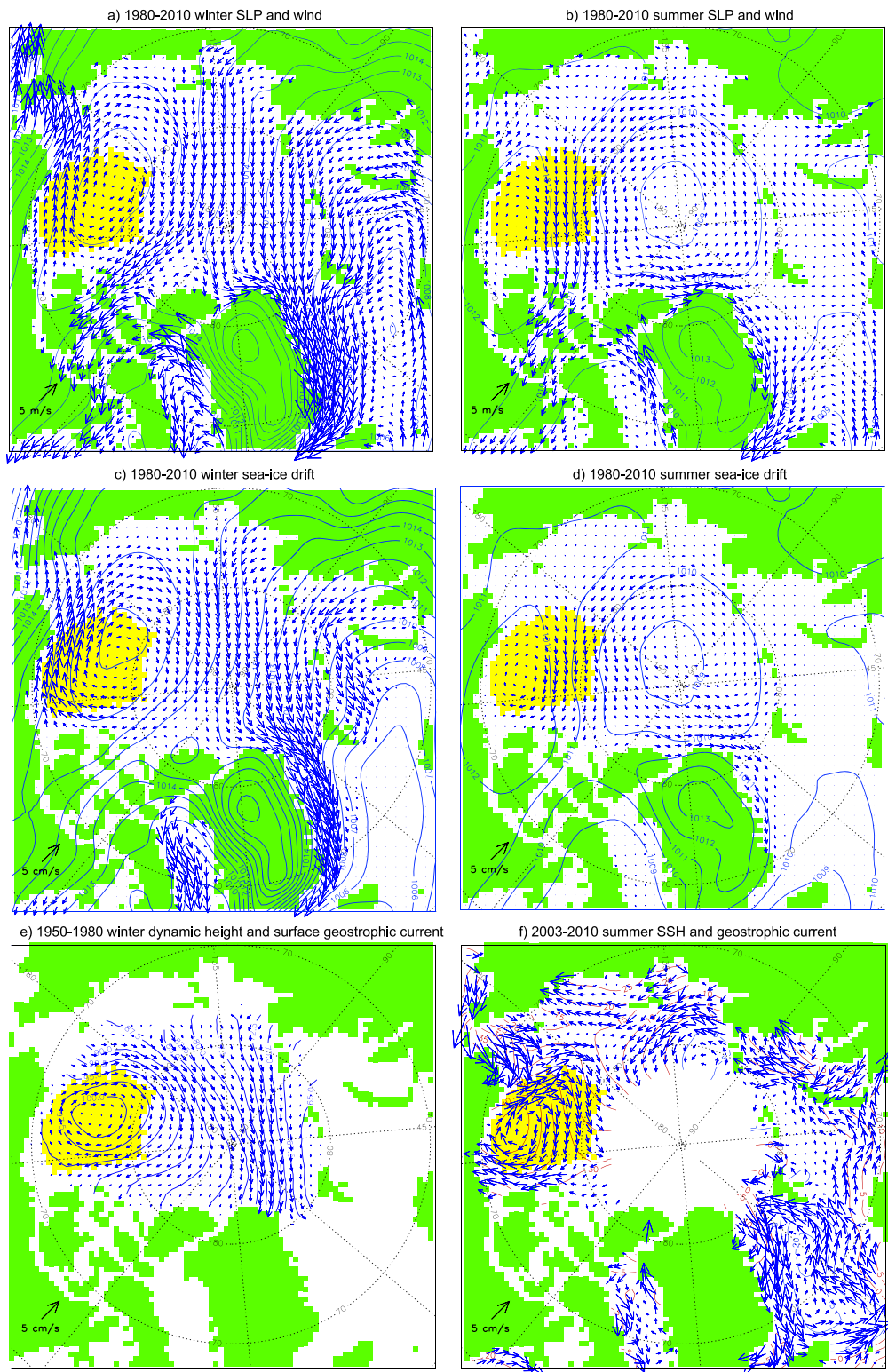


Figure 2. Climatological (1980-2010 mean) (a) winter (October-June) and (b) summer (July-September) sea level pressure (SLP; solid lines, hPa) and geostrophic wind (m/s) in the Arctic Ocean. Data source: National Center for Atmospheric Research/National Centers for Environmental Prediction (NCAR/NCEP) reanalysis 1 (Kalnay et al., 1996). Climatological (1980-2010 mean) sea ice motion in (c) winter and (d) summer. Data source: Polar Pathfinder Daily 25-km EASE-Grid Sea Ice Motion Vectors, Version 4.1 (Tschudi et al., 2019). (e) 1950-1980 mean winter dynamic height (m) and surface geostrophic current (cm/s) based on Timokhov and Tanis (1998). (f) 2003-2014 mean summer sea surface height (cm) and geostrophic current (cm/s) based on Armitage et al. (2016, 2017). The Beaufort Gyre region is shaded yellow.

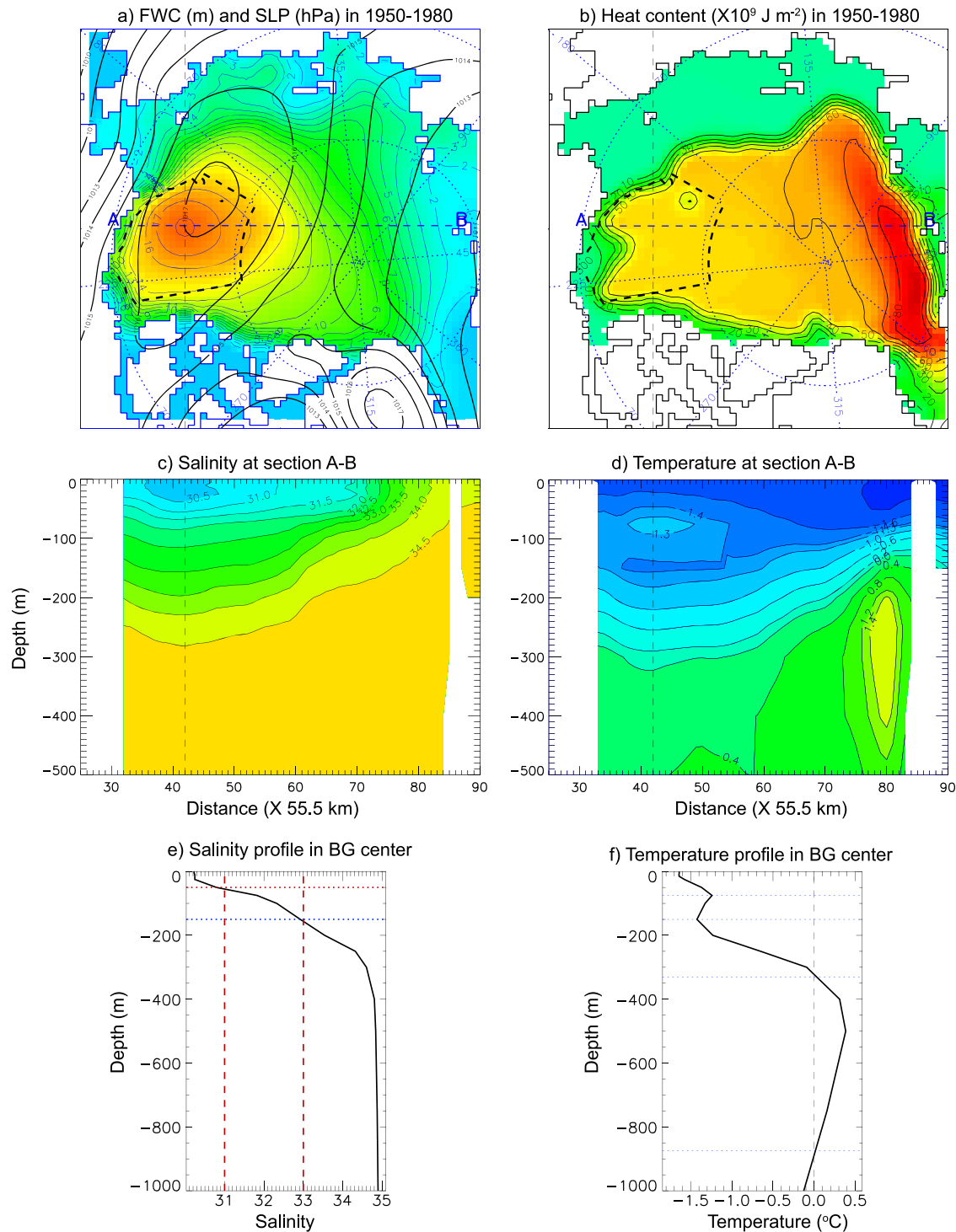


Figure 3. Hydrographic structure of the Beaufort Gyre region. (a) Distribution of freshwater content (m, calculated relative to 34.8 reference salinity) and (b) heat content (right: $\times 10^9 \text{ J/m}^2$, calculated relative to water freezing point). The black contours in (a) indicate the 1950-1980 mean sea level pressure distribution, and the dashed line bounds the Beaufort Gyre region. Vertical sections of (c) salinity and (d) temperature for the transect A-B (marked in panels a and b) through the center of the Beaufort Gyre (maximum freshwater content in a). *T* and *S* climatology are from Timokhov and Tanis (1998). (e) Salinity and (f) temperature profiles in the center of the Beaufort Gyre region illustrate the multilayered structure of the Gyre: mixed layer, Pacific summer and winter waters, Atlantic water layer and deep layers. The vertical dashed lines in (e) bound the Pacific summer water layer located between 31 and 33 salinity and the horizontal dotted lines indicate the shallow and deep bounds of the Pacific summer water layer based on climatology. The horizontal dotted lines in (f) indicate the core of the Pacific summer water (maximum temperature in the upper ocean layer) and the core of the Pacific winter water layer (minimum temperature in the upper ocean layer). The vertical dashed line shows 0°C to identify the upper and lower boundaries of the Atlantic water layer which is defined as having $T > 0^\circ\text{C}$.

and shape from 2003–2014 using satellite data and other environmental parameters determined from observations. The Gyre freshwater content depends on the intensity of the stress curl (a combination of wind and ice stress curls as well as ocean geostrophic flow) at the ocean surface (Proshutinsky, Krishfield, Toole, et al., 2019 this special collection), which does not necessarily coincide with the wind and ice centers of motion shown in Figure 2.

The circulation of Beaufort Gyre subsurface ocean layers (the Pacific summer and winter layers and Atlantic and deep ocean layers) are less well known than the surface layer. In general, it has been shown how the Pacific summer and winter water motion and pathways depend on the atmospheric forcing and sea ice conditions (e.g. Aksenov et al., 2016; Jones, 2001; McLaughlin et al., 2002; Steele et al., 2004; Timmermans et al., 2014). In this special collection, Spall et al. (2018), Zhong et al. (2019), Hirano et al. (2018), and Hu and Myers (2019) discuss the most recent findings associated with the circulation of the Pacific water layers and factors influencing their dynamics and properties.

Past studies suggest that the Atlantic water underlying the Pacific winter water layer most likely circulates cyclonically—in the opposite sense to the shallower layers (e.g., Häkkinen & Mellor, 1992; Karcher et al., 2007, 2012; Nazarenko et al., 1998; Rudels et al., 1994; Treshnikov & Baranov, 1972). Atlantic water heat transport toward the Arctic Ocean is discussed by Muilwijk et al. (2019) in this special collection.

The dynamics of the deep Beaufort Gyre waters are the least well known. Treshnikov and Baranov (1972), who analyzed 1950, 1955, and 1956 winter hydrographic surveys of the Arctic Ocean and calculated currents in this layer employing the Stommel-Koshlyakov model (Koshlyakov, 1961), suggested that below the Atlantic water layer, the deeper layers circulate anticyclonically. Dosser and Timmermans (2017) have interpreted Beaufort Gyre Observing System (BGOS) hydrographic measurements to infer a deep anticyclonic circulation in the Beaufort Gyre.

Several year-long measurements of ocean currents, T and S of the BGOS were recently conducted using McLane Mooring Profiler instruments in the deep (2,600–3,500m) water layers. Timmermans et al. (2010) observed subinertial displacements of isopycnal surfaces in this layer and speculated that these motions are associated with bottom-trapped topographic Rossby waves. Water-column velocity measurements recorded by BGOS McLane Mooring Profilers were concluded to be consistent with the presence of these waves (Zhao & Timmermans, 2018, this special collection).

1.2. Beaufort Gyre Observing System

Many of the studies presented in this special collection center around data collected under BGOS (Figure 1a), which was initiated in 2003 to collect measurements and analyze atmospheric, sea ice, oceanic, and geochemical parameters in the region (Krishfield et al., 2014; Proshutinsky, Krishfield, & Barber, 2009; Proshutinsky, Krishfield, Timmermans, et al., 2009; Proshutinsky et al., 2002; Proshutinsky et al., 2015). As of 2018, 16 years of observations have been obtained, supported by National Science Foundation (NSF), Woods Hole Oceanographic Institution, and the Department of Fisheries and Oceans, Canada (via the Institute of Oceans Sciences) with a large number of other participating institutions. Since the start of the project, an unprecedented data set has been amassed (see the project web site: <http://www.whoi.edu/website/beaufortgyre/data>, and the NSF Arctic Data Center: <https://arcticdata.io/>) with annual time series measurements at more than 30 “standard” locations (Figure 1a). From 2003 to 2018, 1012 CTD profiles at standard locations (Figure 1) and 1155 XCTD profiles between these sites were obtained; 59 moorings were deployed and recovered, 49 Ice-Tethered Profilers, 28 Ice Mass Balance Buoys, 21 Arctic Ocean Flux buoys, 10 O-buoys (recording atmospheric O_3 , CO_2 , and BrO), and 12 Up-Tempo buoys were deployed. Analysis of these data quantifies and documents changes in the Beaufort Gyre system under global warming.

To date, over 160 peer-reviewed publications by authors from many countries and institutions (see Beaufort Gyre website www.whoi.edu/beaufortgyre) including the papers of this special collection have utilized data and results of the Beaufort Gyre Exploration Program (BGEP), which consists of BGOS observations and FAMOS modeling.

These studies have shown that the Arctic Ocean is rapidly changing under global warming. Since 1997, there has been a prevailing anticyclonic atmospheric circulation regime in the Beaufort Gyre region, and this has influenced all physical and biogeochemical variables of the system. The physical changes that occurred in

1948–2013 were examined by Proshutinsky et al. (2015), and the analysis was extended to recent years in this special collection (Proshutinsky, Krishfield, Toole, et al., 2019). Proshutinsky, Krishfield, Toole, et al. (2019) show that the last two decades of sustained anticyclonic wind forcing in the region (1997–2018) differ significantly from the climatology shown in Figure 2. The important consequences of the long-term anticyclonic wind forcing (Figure 2, top panel) are (a) a well-pronounced acceleration of sea ice drift promoted by decreased sea ice concentration with reduced internal ice forces (Figure 2, middle panel) and (b) Ekman transport convergence and Ekman pumping resulting in freshwater content increase and intensification of the geostrophic circulation relative to the climatology (Figure 2, bottom panel).

In addition, it was found that seasonal change in Beaufort Gyre total freshwater content ranges from 5 to 10% of the total freshwater content (depending on the intensity and sense of the atmospheric circulation); inter-annual changes can amount to as much as $1,500 \text{ km}^3$ (around 8% of the total on average); decadal changes were approximately $1,000 \text{ km}^3$ per decade prior to 2000; an accelerated rate of increase of about $4,000 \text{ km}^3$ per decade characterizes the period since 2003; during 2003–2008, the Beaufort Gyre geostrophic circulation has intensified (Armitage et al., 2016, 2017; McPhee, 2013; McPhee et al., 2009); and the baroclinic component of the Transpolar Drift current intensified and shifted toward Canada, accelerating sea-ice drift. Studies in this special collection show that the major causes of Beaufort Gyre freshwater content changes are (i) wind-generated Ekman pumping, (ii) oceanic circulation which influences Ekman pumping via regulation of friction between sea ice and ocean, (iii) eddy dynamics, (iv) ocean mixing accompanied by variability in fresh water available for accumulation, and (v) sea-ice conditions.

While much progress has been made, there are still significant gaps in our understanding of the Beaufort Gyre as an important component of the Arctic climate system. For example, a substantial fraction of freshwater content increase in the Beaufort Gyre region constitutes fresh water that would have otherwise been transported to the North Atlantic. A major outstanding question, addressed in part by Proshutinsky et al. (2015), relates to how this fresh water deficit has influenced and will influence climate of the 21st century. The FAMOS-2 community has recommended investigating how fresh water fluxes from the Beaufort Gyre region influence conditions in the subarctic in context with the increase of fresh meltwater input from Greenland (Dukhovskoy et al., 2019, this special collection).

Other outstanding issues related to Beaufort Gyre freshwater content, which have required modeling approaches, relate to understanding the role of meteoric water (river runoff plus net precipitation; see Lambert et al., 2019, and Kelly, Popova, Aksenov, et al., (2018), and Kelly, Proshutinsky, Popova, et al., (2018), in this special collection) in the observed freshwater content changes, mechanisms for Pacific water transport into the Beaufort Gyre and better understanding of the role of eddies in Beaufort Gyre stabilization (Manucharyan & Isachsen, 2019; and Zhao & Timmermans, 2018, in this special collection).

The set of papers in this special collection fills some of these gaps, tests new hypotheses, and investigates interrelationships among different processes and mechanisms under different atmospheric forcing. In the next section, the results of freshwater content dynamics observed in the Beaufort Gyre region since 2003 are described. Section 3 explores, and sets in context, the major results of the papers published in this special collection.

2. Interannual Changes of Freshwater Content

Estimates of liquid freshwater content in the Beaufort Gyre region based on annual (late summer-early autumn) hydrographic surveys are computed following Proshutinsky, Krishfield, Timmermans, et al. (2009) using CTD, XCTD, and UCTD profiles collected each year from July through October depending on icebreaker availability.

Spatial maps (on a 50-km square grid) of freshwater content distribution were constructed in the Beaufort Gyre region (hereafter, region), which is defined to be between 70 and 81°N , and 130 – 170°W where water depths exceed 300 m, using optimal interpolation for each year from 2003 through 2018 (Figure 4). Uncertainties for each grid cell, determined using the optimal interpolation technique previously described by Proshutinsky, Krishfield, Timmermans, et al. (2009), were updated and are presented in Supporting Information S1. Spatially integrated fresh water volumes for the region (encompassing an area of $1.023 \times$

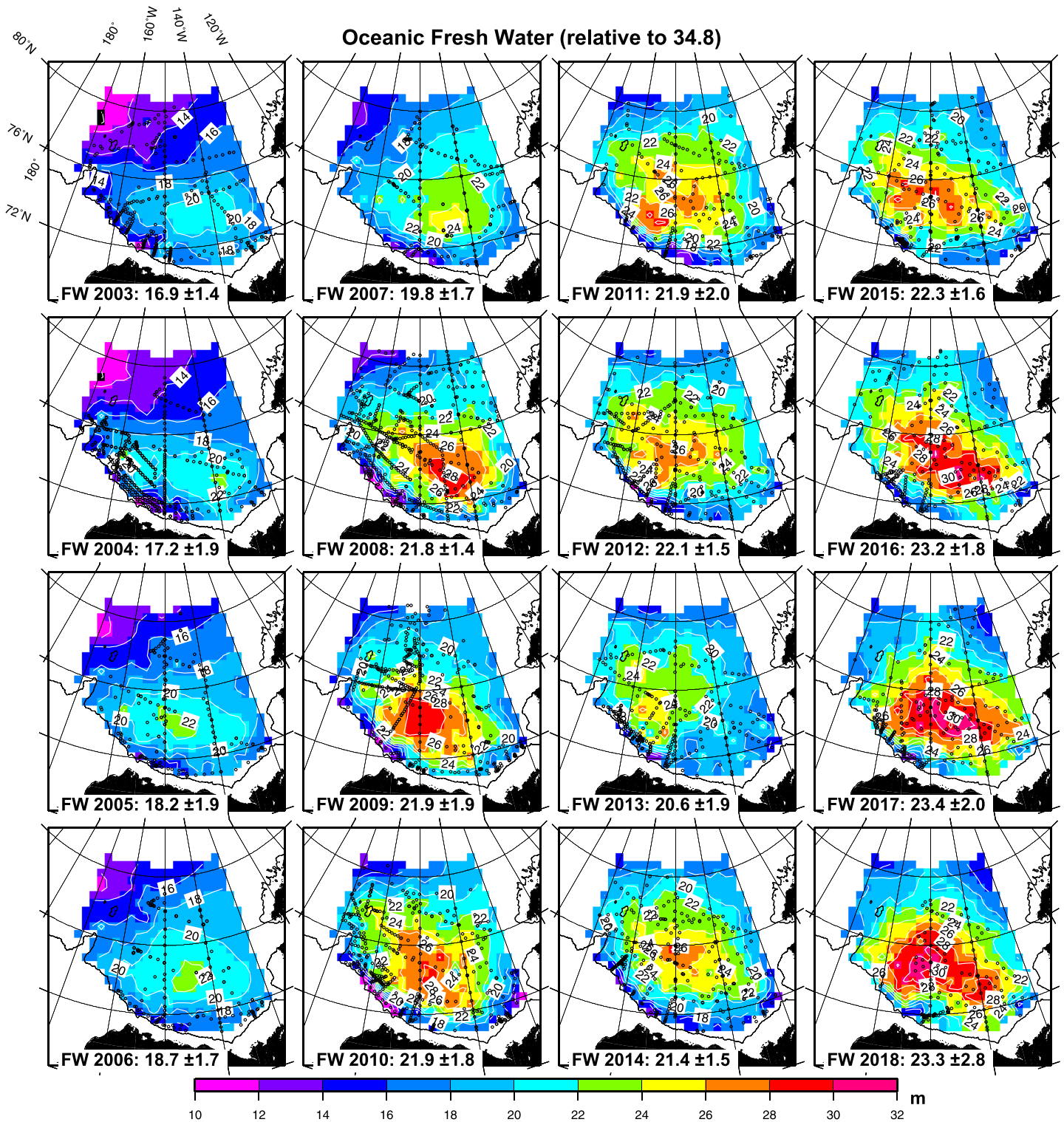


Figure 4. Freshwater content in the Beaufort Gyre region based on hydrographic measurements conducted in July–October. Colors show freshwater content (m), and the black dots indicate locations of observational sites. The white lines duplicate contours of freshwater content distribution shown in colors. Numbers at the bottom of each panel indicate total freshwater content in the region (10^3 km^3) and root-mean-square error of freshwater content interpolation (10^3 km^3).

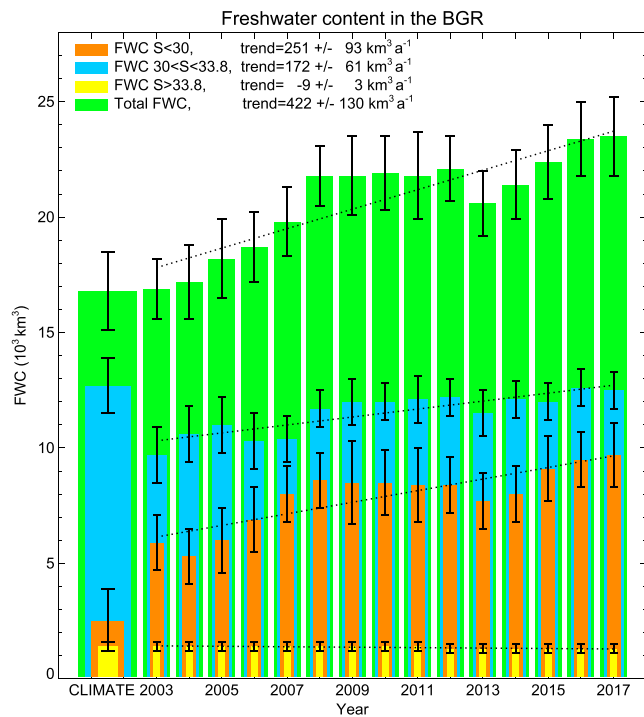


Figure 5. Time series of Beaufort Gyre region freshwater content volume (10^3 km^3) in different layers defined by salinity ranges: deep layer ($S > 33.8$, yellow bars), middle layer ($30 < S < 33.8$, cyan bars), and surface layer ($S < 30$, orange bars). Note that the bars are not stacked, but that the green bars represent total freshwater content. The error bars depict uncertainties in freshwater content estimates. Linear trends (km^3/a) are shown by dotted lines. The left-most wide bars are freshwater content volume derived from summer climatology 1950-1989 (Timokhov & Tanis, 1998). Trend errors are estimated at 95% confidence interval.

910 km^3 , and then decreased to 180 km^3 in 2012 (see Krishfield et al., 2014). Sea-ice freshwater content rebounded temporarily in 2013 to 840 km^3 , before continuing to decrease to 180 km^3 in 2017 and 2018 for an overall negative linear trend of $300 \pm 90 \text{ km}^3$ per decade.

In order to better describe and attribute freshwater content changes, the water column was partitioned into layers bounded by selected isohalines that conditionally encompass: the surface layer containing meteoric and ice melt waters ($S < 30$), a middle layer occupied by Pacific summer and winter waters ($30 < S < 33.8$), and deeper waters largely of Atlantic origin ($33.8 < S < 34.8$). The time series of freshwater content components exhibit interannual changes with significant positive trends in upper and middle layers, while the deep layer's total freshwater content in the 2000s ($\sim 1,400 \text{ km}^3$) was largely unchanged from that of the 1950s-1980s (Figure 5, left "Climate" bar). While there was some redistribution of the relatively small amount of freshwater content in the deep layer from the north to the east and eventually to the south over the 16-year record (not shown), the total decrease in freshwater content was only on the order of 100 km^3 , comparable with the freshwater content uncertainties (all uncertainties are provided in Supporting Information S1-S7). There was also little change in the thickness of this layer over this time (see Supporting Information S7).

From 2003 to 2008, surface layer freshwater content increased from 5,900 to 8,600 km^3 with little change in position of the freshwater content maximum, while the middle layer freshwater content increased from 9,700 to 11,700 km^3 predominantly in the west and north (see Supporting Information S2-S6 for details) where Pacific waters enter the basin (e.g., Timmermans et al., 2014). These freshwater content increases correspond to a mean surface layer thickness increase of approximately 10 m (from 32 to 41 m), and a mean middle layer thickness increase of around 20 m (from 145 to 165 m). Between 2008 and 2012, the surface layer freshwater content and thickness both remained fairly constant; however, middle layer freshwater

10^6 km^3) are labeled for each year on each panel in Figure 4, with uncertainties determined by combining the uncertainties in the profile data with the optimal interpolation errors.

Solid freshwater content volume, referring to fresh water contained in sea ice in the region, was determined using ice draft data from the BGOS moorings in combination with an ice draft parameterization and ice concentrations based on satellite passive microwave data. Full details, including assessment of uncertainties, are provided by Krishfield et al. (2014).

As shown by Proshutinsky, Krishfield, Timmermans, et al. (2009) and discussed by Carmack et al. (2008), the July-October Beaufort Gyre region freshwater content maximum documented by climatology (Figure 1b) shifted southwest after 2003. From 2003 to 2008 (Figure 4), the freshwater content maximum intensified and the total freshwater content increased from 16,900 to 21,800 km^3 over this period. From 2008 to 2012, the total fresh water volume was comparatively steady, although the distribution changed, with a shift in the freshwater content maximum to the west over this period. In 2013, freshwater content decreased from the 2012 value but subsequently resumed increasing in each of the following years, from 20,600 km^3 in 2013 to 23,400 km^3 in 2017 and to 23,300 in 2018. Overall, the regional freshwater content increased by $\sim 40\%$ (i.e., 6,400 km^3) from 2003 to 2018, at a rate of approximately $4,420 \pm 1,300 \text{ km}^3$ per decade. These overall, seasonal, interannual, and longer term fluctuations depend on the complicated interplay of wind, ice, and ocean dynamics and thermodynamics regulating Beaufort Gyre spin-up, dissipation, and stabilization (see for details Kelly, Proshutinsky, Popova et al., 2018; Liang & Losch, 2018; Manucharyan & Isachsen, 2019; Mensa et al., 2018; Regan et al., 2019; and Zhao et al., 2018, etc., in this special collection).

The magnitude of the solid freshwater content in the region and its variability (not shown) are much smaller than the liquid freshwater content.

Between 2003 and 2005, solid freshwater content increased from 610 to

content and layer thickness both increased slightly (by 500 km³ and 10 m, respectively) over this same time period. After a reduction of 700 km³ from 2012 to 2013, surface layer freshwater content showed an increase (by 2,000 km³) through 2017, corresponding to a mean layer thickness increase to 49 m. Over this same period, the middle layer freshwater content decreased by 700 km³ from 2012 to 2013, and then resumed increasing (by 1,000 km³) through 2017, corresponding to a mean layer thickness increase to 178 m (see Supporting Information S7).

Compared to these recent observed properties, the climatology of the 1950s-1980s indicates that the surface layer freshwater content amounted to only 2,500 km³ and was only 14 m thick. The surface layer freshwater content and thickness in 2003 were more than twice the 1950s-1980s values, and by 2017 they had become approximately 4 times greater. On the other hand, the 1950s-1980s middle layer freshwater content (12,700 km³) and thickness (183 m) were both larger than the middle layer freshwater content throughout the 2003-2017 record; middle layer freshwater content and thickness in 2003 were 20-25% smaller than climatological values, but by 2017 were only a few percent less. While surface layer freshwater content properties have shown a significant deviation from climatology, middle layer freshwater content properties have nearly returned to climatological values (although the spatial distribution differs).

3. Beaufort Gyre Phenomenon: Multicomponent System Mechanisms and Changes

The 2003–2018 time series of atmospheric, sea ice, oceanic, and biogeochemistry data, combined with Arctic coupled ice-ocean modeling with atmospheric forcing, have been used to investigate the major causes, consequences, and rates of Beaufort Gyre freshwater accumulation and release (e.g. Doddridge et al., 2019; Manucharyan & Isachsen, 2019; Proshutinsky, Krishfield, Toole, et al., 2009; Regan et al., 2019); identify the major sources of fresh water and the fresh water pathways from the sources to the Beaufort Gyre region (Kelly, Proshutinsky, Popova et al., 2018); explain the major patterns and regimes of the surface, Pacific, and Atlantic water layer circulation (e.g. Hu & Myers, 2019; Spall et al., 2018; Zhong et al., 2019); and reveal the physics of mechanical mixing and convection under the influence of wind, internal wave, and tidal forcing (e.g., Bebieva & Timmermans, 2019; Chanona et al., 2018; Shibley & Timmermans, 2019; Zhao et al., 2018). Other papers in the collection examine the role of sea ice conditions, major features of ice variability, and methods of sea ice prediction in the region (e.g. Babb et al., 2019; Heorton et al., 2019; Lewis & Hutchings, 2019; Mahoney et al., 2019; Yaremchuk et al., 2019). Ecosystem and biogeochemical analyses targeting estimation of biological production rates in both water and sea ice, and characteristics of dissolved organic and inorganic matter, are another focus, with papers employing syntheses of multimodel experiments in combination with collective data analysis (e.g. Dainard et al., 2019; DeGrandpre et al., 2019; Ji et al., 2019; Watanabe et al., 2019).

To explore the Beaufort Gyre in context with the broader Arctic, several papers describe processes of the relationship between the Beaufort Gyre and the northern Pacific and Atlantic Oceans, showing how the Beaufort Gyre region influences, and is influenced by, global climate change including the increase of Greenland melt and modification of Atlantic water circulation (e.g. Dukhovskoy et al., 2019; Muilwijk et al., 2019).

With a focus on modeling, there are several papers that employ a new approach using “climate response functions” to better understand processes of Arctic and subarctic variability and predict future Arctic change (e.g., Brown et al. (2019); Lambert et al., 2019; Muilwijk et al., 2019).

Below, some results of this special collection, with publications organized by discipline, theme, and approach, are briefly summarized.

3.1. Causes and Consequences of Freshwater Content Variability

The causes and consequences of freshwater content changes, discussed in section 2, are extended and developed by Proshutinsky, Krishfield, Toole, et al. (2019) in this special collection. The particular focus of Proshutinsky, Krishfield, Toole, et al. (2019) is an examination of the seasonal and interannual variability using year-round data from Ice-Tethered Profilers (Krishfield et al., 2008; Toole et al., 2011), moorings, and satellite data. It was found that in 2003-2018, the major contributors of fresh water to the Beaufort Gyre were fresh waters coming from Bering Strait and the Mackenzie River.

Results of Proshutinsky, Krishfield, Toole, et al. (2019) are supported by simulations using the 1/12° NEMO model of particles released in the Beaufort Gyre employing a method of backward trajectories to track particle origins (Kelly, Proshutinsky, Popova et al., 2018; this special collection). It was found that pathways of fresh water from Mackenzie and Bering Strait depend significantly on the sense and intensity of the atmospheric circulation, which has been predominantly anticyclonic since 1997. With this forcing, the role of Siberian Rivers as potential fresh water contributors has decreased substantially after the 1990s. A useful numerical study of Pacific water circulation using tracers and freshwater content changes in the upper 200m of the ocean (Hu & Myers, 2019) provides additional information about Pacific water pathway changes, while also comparing results from relatively coarse- vs. high-resolution numerical models. Taken together, the papers above fill many gaps in our understanding of uncertainties in approaches, optimal design of numerical experiments, and effectiveness of Lagrangian and Eulerian methods to track tracer spreading (e.g., Wagner et al., 2019). At least one additional coordinated FAMOS experiment is needed to further develop and compare different approaches for analysis of fresh water composition and circulation in the region under the same forcing and over identical periods of model runs.

The imprint of river runoff variability is examined by Lambert et al. (2019) and Brown et al. (2019) in this special collection. Grivault et al. (2018) evaluate the water transport and volume of fresh water flowing through the straits of the Canadian Arctic Archipelago. Beyond the Beaufort Gyre and Canadian Basin region, freshening of the Arctic Ocean is projected by Shu et al. (2018) using CMIP5 simulations.

3.2. Processes of the Beaufort Gyre Spin-Up and Stabilization

Satellite observations of dynamic ocean topography are used by Regan et al. (2019) to characterize the extent, shape, and location of the Beaufort Gyre beginning in 2003 to 2014. These observations are used to correlate the gyre strength with surface stress. It is found that the strength of Gyre dynamics expressed in the intensity of Dynamic Ocean Topography inferred from satellite data correlates with the surface ocean stress integrated over the previous 3 months. Manucharyan and Isachsen (2019) employ an idealized eddy-resolving model and theoretical formalism to demonstrate that a reduction in diffusivity over continental slopes affects key gyre characteristics and prolongs equilibration. Also in this special collection, Doddridge et al. (2019) theorize that Beaufort Gyre equilibrium is maintained by a balance between the negative feedback between surface currents and ice-ocean stress, wind stress, and eddy diffusivity. Zhao and Timmermans (2018) investigate dynamics of topographic Rossby waves and speculate that their activity is accompanied by kinetic energy dissipation, which plays a role in Beaufort Gyre stabilization. To summarize, a variety of dissipation processes are responsible for balancing wind-energy input and stabilizing the Beaufort Gyre (and therefore also the freshwater content), and better future predictions require quantifying the roles of each factor for different scenarios.

3.3. Eddies and Mixing

Observing, understanding, parameterizing, and explicit modeling of these processes and mechanisms, operating at scales much smaller than the scale of the Beaufort Gyre, are essential for accurate quantification of Beaufort Gyre fresh water accumulation and release mechanisms at all stages from gyre spin-up to stabilization. In this special collection, there are nine papers by FAMOS collaborators that address small-scale processes. Kozlov et al. (2019) provide extensive estimates of surface eddy characteristics in the Beaufort Gyre region. More than 7,500 mesoscale eddies (with mean diameters around 5-6 km) were detected from satellite-borne synthetic aperture radar data over the ice free ocean and in marginal ice zones from June to October of 2007, 2011, and 2016. One interesting result that merits additional analyses is that cyclonic eddies (65% of the total) dominate over anticyclonic eddies in the record. Mesoscale (and submesoscale, around 1-km horizontal scale) dynamics based on surface drifter observations are also analyzed by Mensa et al. (2018) in this issue. It is concluded that without sea ice the major features of these dynamics resemble characteristics in the midlatitudes. The subsurface mesoscale eddy field is studied by Zhao et al. (2018) using horizontal water velocities measured by BGOS moorings. Partitioning of kinetic energy into barotropic and baroclinic modes suggests that the halocline structure plays a specific role in limiting the capacity for frictional dissipation at the sea floor. Double-diffusive mixing and layers in the Beaufort Gyre region are studied by Bebieva and Timmermans (2019) and by Shibley and Timmermans (2019). These papers shed light on the origins of various layer types associated with heat and salt transport, as well as the role of turbulence in limiting double-diffusive heat fluxes. Cole and Stadler (2019) investigate the surface ocean and report a deepening by 9 m

(about 20%) of the winter mixed layer in the Beaufort Gyre region in 2013-2017 relative to 2006-2012 and discuss potential causes for this deepening. Chanona et al. (2018) analyze a large number of conductivity-temperature-pressure profiles to characterize internal wave-driven turbulent dissipation rates; they find a weak seasonal cycle and an absence of interannual variability and trends in the rates of dissipation. While the study indicates that many regions exhibit only weak (molecular) heat fluxes, a set of cases is presented of isolated anomalously large heat fluxes. Finally, Liang and Losch (2018) employ a coupled ice-ocean model to investigate the potential consequences of increased vertical mixing to sea ice conditions and ocean circulation. They show the major effects of increased mixing include reduction of sea ice thickness, weakening of halocline strength, and the formation of cyclonic and anticyclonic water circulation anomalies in different parts of the water column.

3.4. Sea Ice Changes in the Beaufort Gyre

Mechanisms contributing to the significant changes in sea ice in the Beaufort Gyre region are addressed in several papers in this special collection. Babb et al. (2019) discuss seasonal preconditioning toward younger and thinner sea ice during winter 2016 and the influence on summer melt. Heorton et al. (2019) infer sea ice drag coefficients and turning angles from in situ and satellite observations using an inverse modeling framework and conclude that 10-day averaged drag coefficients and turning angles are in agreement with AIDJEX results, further pointing out the importance of correct representation of geostrophic currents, which have intensified significantly after 2003 (Armitage et al., 2017; McPhee, 2013; McPhee et al., 2009). Lewis and Hutchings (2019) examine how sea ice motion is enhanced with the presence of leads, while Mahoney et al. (2019) show how changes in the thickness and circulation of multiyear ice are related to its drift track. Mu et al. (2018) estimate ice thickness in the Arctic Ocean assimilating sea ice data derived from CryoSat-2 satellite into a dynamic ice-ocean model. Yaremchuk et al. (2019) present a study showing advances in short-term forecasting of sea ice conditions in the Beaufort Gyre.

3.5. Ocean Circulation

Circulation patterns of the subsurface ocean layers are addressed in several papers employing both observations and models. The transport of Pacific Water into the Canada Basin and the formation of the Chukchi Slope Current are described by Spall et al. (2019), while Hu and Myers (2019) investigate pathways of Pacific Water in and around the Beaufort Gyre. Kelly, Popova, Aksenov, et al., (2018) employ the use of tracers in the Coupled Model Intercomparison Project Phase 5 (CMIP5) model to ascertain Arctic Ocean pathways of pollutants from Siberian Rivers. Thickening, expansion, and redistribution of the Pacific Winter Water layer are quantified by Zhong et al. (2019). Shu et al. (2018) investigate future changes of freshwater content under influence of different factors including circulation changes in the future.

3.6. Ecosystem and Biogeochemistry Dynamics

Changes in the Beaufort Gyre ecosystem and biogeochemistry have accompanied changes in the physical environment, and dynamics of these systems are addressed in three papers in this special collection. These papers continue long-term work conducted by the FAMOS ecosystem and biogeochemistry group focused on the analyses of acidification, biology, gas exchange, and ecosystem modeling (e.g., Carmack et al., 2010, 2016; Carmack & McLaughlin, 2011; Griffith et al., 2012; Hwang et al., 2008, 2015; Loose et al., 2017; Murata et al., 2008; Nishino et al., 2005, 2009; Smith et al., 2011; Yamamoto-Kawai et al., 2009; Yamamoto-Kawai et al., 2010, 2011). The new papers analyze biological production, distribution of dissolved organic matter (DOM), and inorganic carbon fluxes in the presence of sea ice.

Variations in rates of biological production determined from in situ gas measurements are presented in this special collection by Ji et al. (2019) for the period 2011 to 2016. Interestingly, these authors report that a large increase in total photosynthesis that occurred in 2012, a year of historically low sea ice extent in the Beaufort Gyre, persisted for many years. The data set analyzed in the paper serves as a valuable baseline for future estimates of biological production rates.

Dainard et al. (2019) present DOM absorbance and fluorescence properties in the Canada Basin for 2010-2012. It is found that sea ice reduction observed in 2012 did not influence significantly the DOM composition in the 30-m mixed layer compared to DOM changes observed in 2010.

DeGrandpre et al. (2019) show how inorganic carbon export from the surface layers is related to sea ice formation. Modeling of the ecosystem is performed by Watanabe et al. (2019), who conducted an intercomparison of ice algal productivity in the Chukchi and Barents seas and in the Eurasian and Canada basins at seasonal to decadal scales employing five different models. Similar to previous model intercomparison studies, large differences were found among model results. However, it is reported that since the 1980s, the ice-algal bloom timing shifted to an earlier date and bloom durations shorten in the majority of regions analyzed by Watanabe et al. (2019).

There is a wealth of existing physical, biogeochemical, and ecosystem data collected under the BGOS umbrella that are essential for follow-on studies to those in this special collection. These data and future collections will allow for analyses on topics including meteorological, sea-ice and ocean conditions, ocean turbulence, surface gas exchange in a variety of sea-ice settings, marine bacteria, biological production, microzooplankton, micro-plastics, microbial diversity, methane and nitrous oxide, nitrogen/argon ratios, and many others.

4. Concluding Remarks

The results presented in this special collection have highlighted the vital observations made under the 2003–2018 Beaufort Gyre Exploration Program and employed indispensable collaborations fostered under FAMOS. The studies constitute significant advances in our understanding of change in the Beaufort Gyre region and processes that shape the system's response to change. Taken together, these studies provide compelling motivation for the continuation of the long-term Beaufort Gyre Exploration Program as a fundamental component of the NSF's Arctic Observing Network Program. As the Beaufort Gyre system continues to respond to the varying pressures of climate change, sustained measurements and an engaged scientific community are essential for viable future projections.

Acknowledgments

We would like to thank all FAMOS participants (<https://web.whoi.edu/famos/> and <https://famosarctic.com/>) and collaborators of the Beaufort Gyre Exploration project (<https://www.whoi.edu/beaufortgyre>) for their continued enthusiasm, creativity, and support during all stages of both projects. This research is supported by the National Science Foundation Office of Polar Programs (projects 1845877, 1719280, and 1604085). Any opinions, findings, and conclusions or recommendations expressed in this material are those of the authors and do not necessarily reflect the views of the National Science Foundation. Arctic dynamic topography/geostrophic currents data were provided by the Centre for Polar Observation and Modelling, University College London (www.cpom.ucl.ac.uk/dynamic_topography; Armitage et al. (2016, 2017)). The other data used in this paper are available at the NCAR/NCEP (<https://www.esrl.noaa.gov/psd/data/gridded/data.ncep.reanalysis.html>), NSIDC (<https://nsidc.org/>), NSF's Arctic data center (<https://arcticdata.io/>); Keywords for data search are "Beaufort Gyre", "Krishfield" or "Proshutinsky", and WHOI Beaufort Gyre exploration website (www.whoi.edu/beaufortgyre).

References

- Aagaard, K., & Carmack, E. C. (1989). The role of sea ice and fresh water in the Arctic circulation. *Journal of Geophysical Research*, *94*, 14,485–14,498. <https://doi.org/10.1029/JC094iC10p14485>
- Aksenov, Y., Karcher, M., Proshutinsky, A., Gerdes, R., de Cuevas, B., Golubeva, E., et al. (2016). Arctic pathways of Pacific Water: Arctic Ocean Model Intercomparison experiments. *Journal of Geophysical Research: Oceans*, *121*, 27–59. <https://doi.org/10.1002/2015JC011299>
- Armitage, T. W. K., Bacon, S., Ridout, A. L., Petty, A. A., Wolbach, S., & Tsamados, M. (2017). Arctic Ocean surface geostrophic circulation 2003–2014. *The Cryosphere*, *11*(4), 1767–1780. <https://doi.org/10.5194/tc-11-1767-2017>
- Armitage, T. W. K., Bacon, S., Ridout, A. L., Thomas, S. F., Aksenov, Y., & Wingham, D. J. (2016). Arctic sea surface height variability and change from satellite radar altimetry and GRACE, 2003–2013. *Journal of Geophysical Research: Oceans*, *121*, 4303–4322. <https://doi.org/10.1002/2015JC011579>
- Babb, D. G., Landy, J. C., Barber, D. G., & Galley, R. J. (2019). Winter sea ice export from the Beaufort Sea as a preconditioning mechanism for enhanced summer melt: A case study of 2016. *Journal of Geophysical Research: Oceans*, *124*, 6575–6600. <https://doi.org/10.1029/2019JC015053>
- Bebieva, Y., & Timmermans, M. L. (2019). Double-diffusive layering in the Canada Basin: An explanation of along-layer temperature and salinity gradients. *Journal of Geophysical Research: Oceans*, *124*, 723–735. <https://doi.org/10.1029/2018JC014368>
- Brown, N. J., Nilsson, J., and Pemberton, P. (2019). Arctic Ocean freshwater dynamics: Transient response to increasing river runoff and precipitation. *Journal of Geophysical Research: Oceans*, *124*, 5205–5219. <https://doi.org/10.1029/2018JC014923>
- Carmack, E. C., & McLaughlin, F. A. (2011). Towards recognition of physical and geochemical change in Subarctic and Arctic Seas. *Progress in Oceanography*, *90*(1–4), 90–104. <https://doi.org/10.1016/j.pocean.2011.02.007>
- Carmack, E. C., McLaughlin, F. A., Vagle, S., Melling, H., & Williams, W. J. (2010). Structures and property distributions in the three oceans surrounding Canada in 2007: A basis for a long-term ocean climate monitoring strategy. *Atmosphere-Ocean*, *48*(4), 211–224. <https://doi.org/10.3137/OC324.2010>
- Carmack, E. C., McLaughlin, F. A., Yamamoto-Kawai, M., Itoh, M., Shimada, K., Krishfield, R., & Proshutinsky, A. (2008). Freshwater storage in the Northern Ocean and the special role of the Beaufort Gyre. In R. R. Dickson, J. Meincke, & P. Phines (Eds.), *Arctic–Subarctic Ocean Fluxes, Defining the Role of the Northern Seas in Climate*, (pp. 145–169). Dordrecht, Netherlands: Springer.
- Carmack, E. C., Yamamoto-Kawai, M., Haine, T. W. N., Bacon, S., Bluhm, B. A., Lique, C., et al. (2016). Freshwater and its role in the Arctic Marine System: Sources, disposition, storage, export, and physical and biogeochemical consequences in the Arctic and global oceans. *Journal of Geophysical Research: Biogeosciences*, *121*, 675–717. <https://doi.org/10.1002/2015JG003140>
- Chanona, M., Waterman, S., & Gratton, Y. (2018). Variability of internal wave-driven mixing and stratification in Canadian Arctic shelf and shelf-slope waters. *Journal of Geophysical Research: Oceans*, *123*, 9178–9195. <https://doi.org/10.1029/2018JC014342>
- Cole, S. T., & Stadler, J. (2019). Deepening of the winter mixed layer in the Canada Basin, Arctic Ocean Over 2006–2017. *Journal of Geophysical Research: Oceans*, *124*, 4618–4630. <https://doi.org/10.1029/2019JC014940>
- Condron, A., Winsor, P., Hill, C., & Menemenlis, D. (2009). Simulated response of the Arctic freshwater budget to extreme NAO wind forcing. *Journal of Climate*, *22*(9), 2422–2437. <https://doi.org/10.1175/2008JCLI2626.1>
- Dainard, P., Gueguen, C., Yamamoto-Kawai, M., Williams, W., & Hutchings, J. (2019). Interannual variability in the absorption and fluorescence characteristics of dissolved organic matter in the Canada Basin surface waters. *Journal of Geophysical Research: Oceans*, *124*, 5258–5269. <https://doi.org/10.1029/2018JC014896>

- DeGrandpre, M. D., Lai, C.-Z., Timmermans, M.-L., Krishfield, R. A., Proshutinsky, A., & Torres, D. (2019). Inorganic carbon and pCO₂ variability during ice formation in the Beaufort Gyre of the Canada Basin. *Journal of Geophysical Research: Oceans*, *124*, 4017–4028. <https://doi.org/10.1029/2019JC015109>
- Doddridge, E. W., Meneghello, G., Marshall, J., Scott, J., & Lique, C. (2019). A Three-way balance in the Beaufort Gyre: The Ice-Ocean Governor, wind stress, and eddy diffusivity. *Journal of Geophysical Research: Oceans*, *124*, 3107–3124. <https://doi.org/10.1029/2018JC014897>
- Dosser, H., & Timmermans, M.-L. (2017). Inferring circulation and lateral eddy fluxes in the Arctic Ocean's deep Canada Basin using an inverse method. *Journal of Physical Oceanography*, *48*(2), 245–260. <https://doi.org/10.1175/JPO-D-17-0190.1>
- Dukhovskoy, D., Johnson, M., & Proshutinsky, A. (2004). Arctic decadal variability: An auto-oscillatory system of heat and fresh water exchange. *Geophysical Research Letters*, *31*, L03302. <https://doi.org/10.1029/2003GL019023>
- Dukhovskoy, D., Johnson, M., & Proshutinsky, A. (2006a). Arctic decadal variability from an idealized atmosphere-ice-ocean model: 1. Model description, calibration, and validation. *Journal of Geophysical Research*, *111*(C6), C06028. <https://doi.org/10.1029/2004JC002821>
- Dukhovskoy, D., Johnson, M., & Proshutinsky, A. (2006b). Arctic decadal variability from an idealized atmosphere-ice-ocean model: 2. Simulation of decadal oscillations. *Journal of Geophysical Research*, *111*(C6), C06029. <https://doi.org/10.1029/2004JC002820>
- Dukhovskoy, D. S., Yashayaev, I., Proshutinsky, A., Bamber, J. L., Bashmachnikov, I. L., Chassignet, E. P., et al. (2019). Role of Greenland freshwater anomaly in the recent freshening of the subpolar North Atlantic. *Journal of Geophysical Research: Oceans*, *124*. <https://doi.org/10.1029/2018JC014686>
- Giles, K. A., Laxon, S. W., Ridout, A. L., Wingham, D. J., & Bacon, S. (2012). Western Arctic Ocean freshwater storage increased by wind-driven spin-up of the Beaufort Gyre. *Nature Geoscience*, *5*(3), 194–197. <https://doi.org/10.1038/NGEO1379>
- Griffith, D. R., McNichol, A. P., Xu, L., McLaughlin, F. A., Macdonald, R. W., Brown, K. A., & Eglinton, T. I. (2012). Carbon dynamics in the western Arctic Ocean: Insights from full-depth carbon isotope profiles of DIC, DOC, and POC. *Biogeosciences*, *9*(3), 1217–1224, 2012. www.biogeosciences.net/9/1217/2012/, <https://doi.org/10.5194/bg-9-1217-2012>
- Grivault, N., Hu, X., & Myers, P. G. (2018). Impact of the surface stress on the volume and freshwater transport through the Canadian Arctic Archipelago from a high-resolution numerical simulation. *Journal of Geophysical Research: Oceans*, *123*, 9038–9060. <https://doi.org/10.1029/2018JC013984>
- Haine, T. W. N., Curry, B., Gerdes, R., Hansen, E., Karcher, M., Lee, C., et al. (2015). Arctic freshwater export: Status, mechanisms, and prospects. *Global and Planetary Change*, *125*, 13–35, ISSN 0921-8181. <https://doi.org/10.1016/j.gloplacha.2014.11.013>
- Häkkinen, S., & Mellor, G. L. (1992). Modeling the seasonal variability of the coupled Arctic ice-ocean system. *Journal of Geophysical Research*, *97*(C12), 20,285–20,304. <https://doi.org/10.1029/92JC02037>
- Heorton, H. D. B. S., Tsamados, M., Cole, S. T., Ferreira, A. M. G., Berbellini, A., Fox, M., & Armitage, T. W. K. (2019). Retrieving sea ice drag coefficients and turning angles from in situ and satellite observations using an inverse modeling framework. *Journal of Geophysical Research: Oceans*, *124*, 6388–6413. <https://doi.org/10.1029/2018JC014881>
- Hirano, D., Fukamachi, Y., Ohshima, K. I., Watanabe, E., Mahoney, A. R., Eicken, H., et al. (2018). Winter water formation in coastal polynyas of the eastern Chukchi shelf: Pacific and Atlantic influences. *Journal of Geophysical Research: Oceans*, *123*, 5688–5705. <https://doi.org/10.1029/2017JC013307>
- Hu, X., Myers, P. G. & Lu, Y. (2019). Pacific Water pathway in the Arctic Ocean and Beaufort Gyre in two simulations with different horizontal resolutions. *Journal of Geophysical Research: Oceans*, *124*, 6414–6432. <https://doi.org/10.1029/2019JC015111>
- Hwang, J., Eglinton, T. I., Krishfield, R. A., Manganini, S. J., & Honjo, S. (2008). Lateral organic carbon supply to the deep Canada Basin. *Geophysical Research Letters*, *35*, L11607. <https://doi.org/10.1029/2008GL034271>
- Hwang, J., Kim, M., Manganini, S. J., McIntyre, C. P., Haghipour, N., Park, J. J., et al. (2015). Temporal and spatial variability of particle transport in the deep Arctic Canada Basin. *Journal of Geophysical Research: Oceans*, *120*, 2784–2799. <https://doi.org/10.1002/2014JC010643>
- Ji, B. Y., Sandwith, Z. O., Williams, W. J., Diaconescu, O., Ji, R., Li, Y., et al. (2019). Variations in rates of biological production in the Beaufort Gyre as the Arctic changes: Rates from 2011 to 2016. *Journal of Geophysical Research: Oceans*, *124*, 3628–3644. <https://doi.org/10.1029/2018JC014805>
- Jones, E. P. (2001). Circulation in the Arctic Ocean. *Polar Research*, *20*(2), 139–146. <https://doi.org/10.1111/j.1751-8369.2001.tb00049.x>
- Kalnay, E., Kanamitsu, M., Kistler, R., Collins, W., Deaven, D., Gandin, L., et al. (1996). The NCEP/NCAR 40-year reanalysis project. *Bulletin of the American Meteorological Society*, *77*(3), 437–471. [https://doi.org/10.1175/1520-0477\(1996\)077<0437:TNYRP>2.0.CO;2](https://doi.org/10.1175/1520-0477(1996)077<0437:TNYRP>2.0.CO;2)
- Karcher, M., Kauker, F., Gerdes, R., Hunke, E., & Zhang, J. (2007). On the dynamics of Atlantic Water circulation in the Arctic Ocean. *Journal of Geophysical Research*, *112*, C04S02. <https://doi.org/10.1029/2006JC003630>
- Karcher, M., Smith, J. N., Kauker, F., Gerdes, R., & Smethie, W. Jr. (2012). Recent changes in Arctic Ocean circulation revealed by 129-Iodine observations and modelling. *Journal of Geophysical Research*, *117*, C08007. <https://doi.org/10.1029/2011JC007513>
- Kelly, S., Popova, E., Aksenov, Y., Marsh, R., & Yool, A. (2018). Lagrangian modeling of Arctic Ocean circulation pathways: Impact of advection on spread of pollutants. *Journal of Geophysical Research: Oceans*, *123*, 2882–2902. <https://doi.org/10.1002/2017JC013460>
- Kelly, S. J., Proshutinsky, A., Popova, E. K., Aksenov, Y. K., & Yool, A. (2018). On the origin of water masses in the Beaufort Gyre. *Journal of Geophysical Research: Oceans*, *124*, 4696–4709. <https://doi.org/10.1029/2019JC015022>
- Koshlyakov, M. N. (1961). Calculations of deep ocean circulation. *Oceanology*, *1*(6), 997–1002.
- Kozlov, I. E., Artamonova, A. V., Manucharyan, G. E. & Kubryakov, A. A. (2019). Eddies in the Western Arctic Ocean from spaceborne SAR observations over open ocean and marginal ice zones. *Journal of Geophysical Research: Oceans*, *124*, 6601–6616. <https://doi.org/10.1029/2019JC015113>
- Krishfield, R., Toole, J., Proshutinsky, A., & Timmermans, M.-L. (2008). Automated Ice-Tethered Profilers for seawater observations under pack ice in all seasons. *Journal of Atmospheric and Oceanic Technology*, *25*(11), 2091–2105. <https://doi.org/10.1175/2008JTECH0587.1>
- Krishfield, R. A., Proshutinsky, A., Tateyama, K., Williams, W. J., Carmack, E. C., McLaughlin, F. A., & Timmermans, M.-L. (2014). Deterioration of perennial sea ice in the Beaufort Gyre from 2003 to 2012 and its impact on the oceanic freshwater cycle. *Journal of Geophysical Research: Oceans*, *119*, 1271–1305. <https://doi.org/10.1002/2013JC008999>
- Lambert, E., Nummelin, A., Pemberton, P., & Ilıcak, M. (2019). Tracing the imprint of river runoff variability on Arctic water mass transformation. *Journal of Geophysical Research: Oceans*, *124*, 302–319. <https://doi.org/10.1029/2017JC013704>
- Lewis, B. J., & Hutchings, J. K. (2019). Leads and associated sea ice drift in the Beaufort Sea in winter. *Journal of Geophysical Research: Oceans*, *124*, 3411–3427. <https://doi.org/10.1029/2018JC014898>
- Lewis, E. L. (Ed) (2000). *The freshwater budget of the Arctic Ocean*, (p. 623). Dordrecht: Kluwer Academic Publishers, xxii +. <https://doi.org/10.1017/S003224740001713>

- Liang, X., & Losch, M. (2018). On the effects of increased vertical mixing on the Arctic Ocean and sea ice. *Journal of Geophysical Research: Oceans*, *123*, 9266–9282. <https://doi.org/10.1029/2018JC014303>
- Lique, C., Holland, M. M., Dibike, Y. B., Lawrence, D. M., & Screen, J. A. (2016). Modeling the Arctic freshwater system and its integration in the global system: Lessons learned and future challenges. *Journal of Geophysical Research: Biogeosciences*, *121*, 540–566. <https://doi.org/10.1002/2015JG003120>
- Loose, B., Kelly, R. P., Bigdeli, A., Williams, W., Krishfield, R., Rutgers van der Loeff, M., & Moran, S. B. (2017). How well does wind speed predict air-sea gas transfer in the sea ice zone? A synthesis of radon deficit profiles in the upper water column of the Arctic Ocean. *Journal of Geophysical Research: Oceans*, *122*, 3696–3714. <https://doi.org/10.1002/2016JC012460>
- Mahoney, A. R., Hutchings, J. K., Eicken, H., & Haas, C. (2019). Changes in the thickness and circulation of multiyear ice in the Beaufort Gyre determined from pseudo-Lagrangian methods from 2003–2015. *Journal of Geophysical Research: Oceans*, *124*, 5618–5633. <https://doi.org/10.1029/2018JC014911>
- Manucharyan, G. E., & Isachsen, P. E. (2019). Critical role of continental slopes in halocline and eddy dynamics of the Ekman-driven Beaufort Gyre. *Journal of Geophysical Research: Oceans*, *124*, 2679–2696. <https://doi.org/10.1029/2018JC014624>
- Marshall, J., Scott, J., & Proshutinsky, A. (2017). Climate Response Functions for the Arctic Ocean: a proposed coordinated modeling experiment. In *Geoscientific Model Development Discussion*, (pp. 2833–2848). <https://doi.org/10.5194/gmd-10-2833-2017>
- McLaughlin, F., Carmack, E., Krishfield, R., Guay, C., Yamamoto-Kawai, M., Itoh, M., et al. (2011). The changing status of the Canada Basin: From Bellwether to Alarm Bells in the 21st century. *Oceanography*, *24*, 146–159. <https://doi.org/10.5670/oceanog.2011.66>
- McLaughlin, F., Carmack, E., Macdonald, R., Weaver, A. J., & Smith, J. (2002). The Canada Basin, 1989–1995: Upstream events and far-field effects of the Barents Sea. *Journal of Geophysical Research*, *107*(C7), 3082. <https://doi.org/10.1029/2001JC000904>
- McPhee, M. G. (2013). Intensification of geostrophic currents in the Canada Basin, Arctic Ocean. *Journal of Climate*, *26*, 3130–3138. <https://doi.org/10.1175/JCLI-D-12-00289.1>
- McPhee, M. G., Proshutinsky, A., Morison, J. H., Steele, M., & Alkire, M. B. (2009). Rapid change in freshwater content of the Arctic Ocean. *Geophysical Research Letters*, *36*, L10602. <https://doi.org/10.1029/2009GL37252>
- Mensa, J. A., Timmermans, M.-L., Kozlov, I. E., Williams, W. J., & Özgökmen, T. M. (2018). Surface drifter observations from the Arctic Ocean's Beaufort Sea: Evidence for submesoscale dynamics. *Journal of Geophysical Research: Oceans*, *123*, 2635–2645. <https://doi.org/10.1002/2017JC013728>
- Mu, L., Losch, M., Yang, Q., Ricker, R., Losa, S. N., & Nerger, L. (2018). Arctic-wide sea ice thickness estimates from combining satellite remote sensing data and a dynamic ice-ocean model with data assimilation during the CryoSat-2 period. *Journal of Geophysical Research: Oceans*, *123*, 7763–7780. <https://doi.org/10.1029/2018JC014316>
- Muilwijk, M., M. Ilicak, S. B. Cornish, S. Danilov, R. Gelderloos, R. Gerdes, et al. (2019). Arctic Ocean response to Greenland Sea wind anomalies in a suite of model simulations. *Journal of Geophysical Research: Oceans*, *124*, 6286–6322. <https://doi.org/10.1029/2019JC015101>
- Murata, A., Shimada, K., Nishino, S., & Itoh, M. (2008). Distributions of surface water CO₂ and air-sea flux of CO₂ in coastal regions of the Canadian Beaufort Sea in late summer. *Biogeosciences Discussions*, *5*, 5093–5132. <https://doi.org/10.5194/bgd-5-5093-2008>
- Nazarenko, L., Holloway, G., & Tausnev, N. (1998). Dynamics of transport of “Atlantic signature” in the Arctic Ocean. *Journal of Geophysical Research*, *103*(C13), 31,003–31,015. <https://doi.org/10.1029/1998JC900017>
- Nishino, S., Shimada, K., & Itoh, M. (2005). Use of ammonium and other nitrogen tracers to investigate the spreading of shelf waters in the western Arctic halocline. *Journal of Geophysical Research*, *110*, C10005. <https://doi.org/10.1029/2003JC002118>
- Nishino, S., Shimada, K., Itoh, M., & Chiba, S. (2009). Vertical double silicate maxima in the sea-ice reduction region of the western Arctic Ocean: Implications for an enhanced biological pump due to sea-ice reduction. *Journal of Oceanography*, *65*, 871–883. <https://doi.org/10.1007/s10872-009-0072-2>
- Nummelin, A., Ilicak, M., Li, C., & Smedsrud, L. H. (2016). Consequences of future increased Arctic runoff on Arctic Ocean stratification, circulation, and sea ice cover. *Journal of Geophysical Research: Oceans*, *121*, 617–637. <https://doi.org/10.1002/2015JC011156>
- Overland, J. E. (2009). Meteorology of the Beaufort Sea. *Journal of Geophysical Research*, *114*, C00A07. <https://doi.org/10.1029/2008JC004861>
- Proshutinsky, A., Aksenov, Y., Holland, D., Kinney, J. C., Gerdes, R., Holloway, G., et al. (2011). Arctic Ocean change studies: synthesizing model results and observations. *Oceanography*, *24*, 102–113. <https://doi.org/10.5670/oceanog.2011.61>
- Proshutinsky, A., Bourke, R. H., & McLaughlin, F. A. (2002). The role of the Beaufort Gyre in Arctic climate variability: Seasonal to decadal climate scales. *Geophysical Research Letters*, *29*(23), 2100. <https://doi.org/10.1029/2002GL015847>
- Proshutinsky, A., Dukhovskoy, D., Timmermans, M.-L., Krishfield, R., & Bamber, J. (2015). Arctic circulation regimes. *Philosophical Transactions of the Royal Society A*, *373*, 20140160. <https://doi.org/10.1098/rsta.2014.0160>
- Proshutinsky, A., Krishfield, R., & Barber, D. (2009). Preface to special section on Beaufort Gyre Climate System Exploration Studies: Documenting key parameters to understand environmental variability. *Journal of Geophysical Research*, *114*, C00A08. <https://doi.org/10.1029/2008JC005162>
- Proshutinsky, A., Krishfield, R., Timmermans, M.-L., Toole, J., Carmack, E., McLaughlin, F., et al. (2009). Beaufort Gyre freshwater reservoir: State and variability from observations. *Journal of Geophysical Research*, *114*, C00A10. <https://doi.org/10.1029/2008JC005104>
- Proshutinsky, A., Krishfield, R., Toole, J.M., Timmermans, M.L., Williams, W., Zimmermann, S., et al. (2019). Analysis of the Beaufort Gyre freshwater content in 2003–2018. *Journal of Geophysical Research: Oceans*, *124*, 9657–9688. <https://doi.org/10.1029/2019JC015281>
- Rabe, B., Karcher, M., Kauker, F., Schauer, U., Toole, J. M., Krishfield, R. A., et al. (2014). Arctic Ocean basin liquid freshwater storage trend 1992–2012. *Geophysical Research Letters*, *41*, 961–968. <https://doi.org/10.1002/2013GL058121>
- Rabe, B., Karcher, M., Schauer, U., Toole, J., Krishfield, R., Pisarev, S., et al. (2011). An assessment of Arctic Ocean freshwater content changes from the 1990s to 2006–2008. *Deep-Sea Research Part I*, *58*, 173–185. <https://doi.org/10.1016/j.dsr.2010.12.002>
- Regan, H. C., Lique, C., & Armitage, T. W. K. (2019). The Beaufort Gyre extent, shape, and location between 2003 and 2014 from satellite observations. *Journal of Geophysical Research: Oceans*, *124*, 844–862. <https://doi.org/10.1029/2018JC014379>
- Rudels, B., Jones, E. P., Anderson, L. G., & Kattner, G. (1994). On the intermediate depth waters of the Arctic Ocean. In O. M. Johannessen, R. D. Muench, & J. E. Overland (Eds.), *The Polar Oceans and Their Role in Shaping the Global Environment: The Nansen Centennial Volume*, *Geophys. Monogr., No. 85*, *Amer. Geophys. Union*, 33–46. <https://doi.org/10.1029/GM085p0033>
- Shibley, N. C., & Timmermans, M.-L. (2019). The formation of double-diffusive layers in a weakly turbulent environment. *Journal of Geophysical Research: Oceans*, *124*, 1445–1458. <https://doi.org/10.1029/2018JC014625>
- Shu, Q., Qiao, F., Song, Z., Zhao, J., & Li, X. (2018). Projected freshening of the Arctic Ocean in the 21st century. *Journal of Geophysical Research: Oceans*, *123*, 9232–9244. <https://doi.org/10.1029/2018JC014036>

- Smith, J. N., McLaughlin, F. A., Smethie, W. M. Jr., Moran, S. B., & Hagstrom, K. (2011). 129I, 137Cs and CFC-11 Tracer transit time distributions in the Arctic Ocean. *Journal of Geophysical Research*, *116*, C04024. <https://doi.org/10.1029/2010JC006471>
- Spall, M., Pickart, R., Li, M., Itoh, M., Lin, P., Kikuchi, T., & Qi, Y. (2018). Transport of Pacific water into the Canada Basin and the formation of the Chukchi Slope Current. *Journal of Geophysical Research: Oceans*, *123*, 7453–7471. <https://doi.org/10.1029/2018JC013825>
- Steele, M., Ermold, W., Häkkinen, S., Holland, D., Holloway, G., Karcher, M., et al. (2001). Adrift in the Beaufort Gyre: A model inter-comparison. *Geophysical Research Letters*, *28*(15), 2935–2938. <https://doi.org/10.1029/2001GL012845>
- Steele, M., Morison, J., Ermold, W., Rigor, I., Ortmeyer, M., & Shimada, K. (2004). Circulation of summer Pacific halocline water in the Arctic Ocean. *Journal of Geophysical Research*, *109*, C02027. <https://doi.org/10.1029/2003JC002009>
- Timmermans, M.-L., Proshutinsky, A., Golubeva, E., Jackson, J. M., Krishfield, R. M., McCall, M., et al. (2014). Mechanisms of Pacific Summer Water variability in the Arctic's Central Canada Basin. *Journal of Geophysical Research: Oceans*, *119*, 7523–7548. <https://doi.org/10.1002/2014JC01027>
- Timmermans, M.-L., Proshutinsky, A., Krishfield, R. A., Perovich, D. K., Richter-Menge, J. A., Stanton, T. P., & Toole, J. M. (2011). Surface freshening in the Arctic Ocean's Eurasian Basin: An apparent consequence of recent change in the wind-driven circulation. *Journal of Geophysical Research*, *116*, C00D03. <https://doi.org/10.1029/2011JC006975>
- Timmermans, M.-L., Rainville, L., Thomas, L., & Proshutinsky, A. (2010). Moored observations of bottom-intensified motions in the deep Canada Basin, Arctic Ocean. *Journal of Marine Research*, *68*, 625–641. <https://doi.org/10.1357/002224010794657137>
- Timokhov, L., & Tanis F. (1998). Joint U.S.-Russian Atlas of the Arctic Ocean [CD-ROM], *Environ. Res. Inst. of Mich.*, Ann Arbor, Mich.
- Toole, J. M., Krishfield, R. A., Timmermans, M.-L., & Proshutinsky, A. (2011). The Ice-Tethered Profiler: Argo of the Arctic. *Oceanography*, *24*, 126–135. <https://doi.org/10.5670/oceanog.2011.64>
- Treshnikov, A. F., & Baranov, G. I. (1972). *Water circulation in the Arctic Basin*, (p. 145). Leningrad: Gidrometeoizdat. translated from Russian, Jerusalem, 1973
- Tschudi, M., Fowler, C., Maslanik, J., Stewart, J. S., & Meier, W. (2019). *Polar Pathfinder Daily 25 km EASE-Grid Sea Ice Motion Vectors, Version 4*. Boulder, Colorado USA: NASA National Snow and Ice Data Center Distributed Active Archive Center. <https://doi.org/10.5067/O57VAIT2AYYY> [May 2019]
- Wagner, P., Rühls, S., Schwarzkopf, F. U., Koszalka, I. M., & Biastoch, A. (2019). Can Lagrangian Tracking Simulate Tracer Spreading in a High-Resolution Ocean General Circulation Model? *Journal of Physical Oceanography*, *49*, 1141–1157. <https://doi.org/10.1175/JPO-D-18-0152.1>
- Watanabe, E., Jin, M., Hayashida, J., & Zhang, J. & Steiner, N. (2019). Can Lagrangian Multi-model intercomparison of the Pan-Arctic ice-algal productivity on seasonal, interannual, and decadal timescales *Journal of Geophysical Research: Oceans*, *124*, 9052–9083, <https://doi.org/10.1029/2019JC015100D-18-0152.1>
- Yamamoto-Kawai, M., Carmack, E. C., McLaughlin, F. A., & Falkner, K. K. (2010). Oxygen isotope ratio, barium and salinity in waters around the North American coast from the Pacific to the Atlantic: Implications for freshwater sources to the Arctic throughflow. *Journal of Marine Research*, *68*, 97–117. <https://doi.org/10.1357/002224010793078988>
- Yamamoto-Kawai, M., McLaughlin, F., Carmack, E., Nishino, S., & Shimada, K. (2009). Aragonite undersaturation in the Arctic Ocean: Effects of ocean acidification and sea ice melt. *Science*, *326*, 1098–1100. <https://doi.org/10.1126/science.1174190>
- Yamamoto-Kawai, M., McLaughlin, F. A., & Carmack, E. C. (2011). Effects of ocean acidification, warming and melting of sea ice on aragonite saturation of the Canada Basin surface water. *Geophysical Research Letters*, *38*, L03601. <https://doi.org/10.1029/2010GL045501>
- Yaremchuk, M., Townsend, T., Pantelev, G., Hebert, D., & Allard, R. (2019). Advancing short-term forecasts of ice conditions in the Beaufort Sea. *Journal of Geophysical Research: Oceans*, *124*, 807–820. <https://doi.org/10.1029/2018JC014581>
- Zhao, B., & Timmermans, M.-L. (2018). Topographic Rossby waves in the Arctic Ocean's Beaufort Gyre. *Journal of Geophysical Research: Oceans*, *123*, 6521–6530. <https://doi.org/10.1029/2018JC014233>
- Zhao, M., Timmermans, M.-L., Krishfield, R., & Manucharyan, G. (2018). Partitioning of kinetic energy in the Arctic Ocean's Beaufort Gyre. *Journal of Geophysical Research: Oceans*, *123*, 4806–4819. <https://doi.org/10.1029/2018JC014037>
- Zhong, W., Steele, M., Zhang, J., & Cole, S. T. (2019). Circulation of Pacific Winter Water in the western Arctic Ocean. *Journal of Geophysical Research: Oceans*, *124*, 863–881. <https://doi.org/10.1029/2018JC014604>